

Eu(III)-Functionalized MIL-124 as Fluorescent Probe for Highly Selectively Sensing Ions and Organic Small Molecules Especially for Fe(III) and Fe(II)

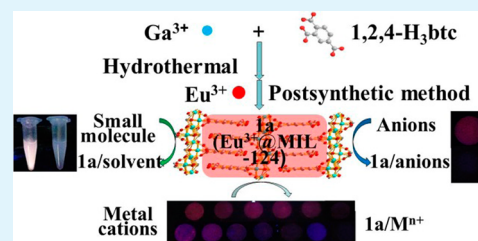
Xiao-Yu Xu and Bing Yan*

Department of Chemistry, Tongji University, Shanghai 200092, China

S Supporting Information

ABSTRACT: A layerlike MOF (MIL-124, or $\text{Ga}_2(\text{OH})_4(\text{C}_9\text{O}_6\text{H}_4)$) has been prepared and chosen as a parent compound to encapsulate Eu^{3+} cations by one uncoordinated carbonyl group in its pores. The Eu^{3+} -incorporated sample (Eu^{3+} @MIL-124) is fully characterized, which shows excellent luminescence and good fluorescence stability in water or other organic solvents. Subsequently, we choose Eu^{3+} @MIL-124 as sensitive probe for sensing metal ions, anions, and organic small molecules because of its robust framework. Studying of the luminescence properties reveals that the complex Eu^{3+} @MIL-124 was developed as a highly selective and sensitive probe for detection of Fe^{3+} (detection limit, $0.28 \mu\text{M}$) and Fe^{2+} ions through fluorescence quenching of Eu^{3+} and MOF over other metal ions. In connection to this, a probable sensing mechanism was also discussed in this paper. In addition, when Eu^{3+} @MIL-124 was immersed in the different anions solutions and organic solvents, it also shows highly selective for $\text{Cr}_2\text{O}_7^{2-}$ (detection limit, $0.15 \mu\text{M}$) and acetone. Remarkably, it is the first Eu-doped MOF to exhibit an excellent ability for the detection of Fe^{3+} and Fe^{2+} in an aqueous environment without any structural disintegration of the framework.

KEYWORDS: Eu^{3+} @MIL-124, fluorescent probe, Fe^{3+} and Fe^{2+} sensing, sensing mechanism, aqueous environment, $\text{Cr}_2\text{O}_7^{2-}$ and acetone sensing



INTRODUCTION

As the most abundant transition metal in cellular systems,¹ iron, presenting in both Fe(II) and Fe(III), plays an indispensable role in many biological processes because it widely exists in the structures of numerous enzymes, proteins, and transcriptional events.^{2–8} Either its deficiency or excess can disturb cellular homeostasis and metabolism. The damages to cells may further result in many kinds of disease, such as hepatitis, cancer, neurodegenerative Alzheimer's disease, and Parkinson's disease.¹ Therefore, selective detection or sensing of iron over other metal ions seems to be very important for human health. In fact, many works have successfully reported the sensing of Fe^{3+} .^{9–12} However, there are only a few fluorescent sensors that select Fe^{2+} over Fe^{3+} , pyrene-TEMPO, DansSQ, and BPD-Cy-Tpy,^{13–15} all of which are small molecule sensors. Selective sensing of Fe^{3+} and Fe^{2+} , simultaneously, without the interference of other mixed metal ions through fluorescence quenching is still a challenge now.

Over the last two decades, extensive efforts on metal–organic frameworks (MOFs), a family of porous materials constructed by the assembly of metal-containing units with appropriate organic linking groups, have led to not only the creation of a huge number of diverse topologies with aesthetic beauty but also to some important applications, such as gas storage,^{16–20} separation,^{21–24} heterogeneous catalysis,^{25,26} sensing,^{27–32} and drug delivery.^{33,34} Among the large number of MOFs, Ln-MOFs have been receiving increasing attention because they

are useful for the development of sensing technologies, among other applications. It needs to be referred that the potential application in fluorescence sensors of Ln-MOFs becomes attractive because of their virtues of high color purity, high luminescence quantum efficiencies, and a wide range of lifetimes.³⁵ The pioneering work by the Chen group has focused on various Ln-MOFs materials for the sensing and detection of various metal ions, anions, and small molecules, including Cu^{2+} , F^- , acetone, DNT, and so on.^{36–39} Besides, considerable efforts have been focused on the detection of Zn^{2+} , Mg^{2+} , Ag^+ , Cu^{2+} , and Fe^{3+} ions based on Ln-MOFs.^{40–45} To date, several mechanisms have been explored for metal–ligand coordination interaction (weak binding of metal ions to heteroatom (N or O) within the ligands) and intramolecular energy transfer from the ligand to metal ion.^{46–49} Recently, an alternative strategy to construct lanthanide-based MOFs is by postsynthetic method (PSM) whose chemical modification can be performed on the fabricated material rather than on molecule precursors.⁴⁰ An increasing number of Ln-doped MOFs, such as Al-MIL-53-COOH, MIL-121, MIL-53, and MOF-76,^{50–52} have been used as luminescence probes to detect metal ions, anions, and organic small molecules.

Received: October 14, 2014

Accepted: December 16, 2014

Published: December 16, 2014

Stimulated by this, herein we choose a lanthanide-doped MOFs prepared by PSM as the luminescent sensor.

In our context, performing a layerlike structure, MIL-124 ($\text{Ga}_2(\text{OH})_4(\text{C}_9\text{O}_6\text{H}_4)$) was prepared through a facile hydrothermal approach and chosen as a parent framework. A new class of lanthanide-doped luminescence MOFs was obtained through encapsulating Eu^{3+} cations in MIL-124, which shows the high thermal and chemical stabilities. What is more, Eu^{3+} @MIL-124 was developed as highly selective and sensitive fluorescence probe targeting Fe^{3+} and Fe^{2+} ions in aqueous solutions. That can be probed by the fact that they have different quenching effect to Eu^{3+} and MIL-124. The possible sensing mechanisms toward to Fe^{3+} and Fe^{2+} were also discussed in detail. In addition, the Eu^{3+} @MIL-124 has also been chosen as a fluorescence probe to sensing anions and organic small molecule. The results indicate that both anions and organic small molecule have fluorescence quenching effect to Eu^{3+} @MIL-124, especially in the case of $\text{Cr}_2\text{O}_7^{2-}$ and acetone, which will cause adverse effects on human health and environment. The color changing can be observed by naked eyes under the UV-light irradiation. As expected, Eu^{3+} @MIL-124 is suitable for becoming one fluorescence probe with high selective.

EXPERIMENTAL SECTION

Synthesis of MIL-124. MIL-124 was hydrothermal synthesized from a mixture of $\text{Ga}(\text{NO}_3)_3 \cdot x\text{H}_2\text{O}$ (0.6 g, 2.4 mmol), 1,2,4- H_3btc (0.37 g, 1.8 mmol), and H_2O (5 mL, 227.8 mmol) described in the literature.¹⁷ The mixture was further stirred 30 min before transferring the resulting suspension to a Teflon-lined steel autoclave, and then heated at 210 °C for 24 h. The initial and final pH values were 0.4 and 0.6, respectively. The white powered solid were collected by centrifugation at 13 000 rpm for 5 min, washed three times with deionized water, and dried at 100 °C for 24 h.

Preparation of Eu^{3+} @MIL-124. Eu^{3+} @MIL-124 was prepared by soaking MIL-124 (100 mg) into the ethanol solution of $\text{EuCl}_3 \cdot 6\text{H}_2\text{O}$ (10 mL, 2 mmol) for 2 days. After separating by centrifugation and washing with ethanol to remove residual Eu^{3+} , the resulting white powder was dried under a vacuum at 80 °C for 6 h.

Luminescence Sensing Experiment. Eu^{3+} @MIL-124/M or Eu^{3+} @MIL-124/anion was prepared by introducing Eu^{3+} @MIL-124 power (2 mg) into aqueous solution (2 mL, 1×10^{-2} molL⁻¹) of MCl_x ($\text{M}^{n+} = \text{K}^+, \text{Na}^+, \text{Hg}^{2+}, \text{Cd}^{2+}, \text{Ca}^{2+}, \text{Ni}^{2+}, \text{Co}^{2+}, \text{Mn}^{2+}, \text{Cu}^{2+}, \text{Fe}^{2+}, \text{Al}^{3+}, \text{Fe}^{3+}$) or anion (anion = $\text{F}^-, \text{Cl}^-, \text{Br}^-, \text{I}^-, \text{NO}_3^-, \text{SO}_4^{2-}, \text{CrO}_4^{2-}, \text{Cr}_2\text{O}_7^{2-}$) at room temperature. For the experiments of sensing small molecules, 2 mg Eu^{3+} @MIL-124 was immersed in same amounts (2 mL) of small molecules solvents. The mixtures were then used for luminescence measurements. The luminescence data were collected after 5 min.

Materials and Instrumentation. All the solvents and reagents (analytical grade and spectroscopic grade) were obtained commercially and used as received. Gallium nitrate hydrate ($\text{Ga}(\text{NO}_3)_3 \cdot x\text{H}_2\text{O}$, 99.9%) and 1,2,4-benzenetricarboxylic acid (noted 1,2,4- H_3btc , $\text{C}_6\text{H}_3(\text{CO}_2\text{H})_3$, 99%) were used to synthesize MIL-124 bought from Aldrich. The salts of $\text{EuCl}_3 \cdot 6\text{H}_2\text{O}$ were prepared by dissolving Eu_2O_3 into excess hydrochloric acid (37%). Aqueous solutions of $\text{K}^+, \text{Na}^+, \text{Hg}^{2+}, \text{Cd}^{2+}, \text{Ca}^{2+}, \text{Ni}^{2+}, \text{Co}^{2+}, \text{Mn}^{2+}, \text{Al}^{3+}, \text{Cu}^{2+}$, and Fe^{3+} were prepared from chlorate salts; Fe^{2+} solution was prepared from ferrous chloride and used immediately. PXRD patterns were obtained on a Bruker D8 diffractometer using $\text{Cu K}\alpha$ radiation with 40 mA and 40 kV and the dates were collected within the 2θ range of 5–50°. Scanning electronic microscope (SEM) images were recorded with a Hitachi S-4800. Fourier transform infrared (FTIR) spectra were recorded in the range 4000–400 cm^{-1} on a Nexus 912 AO446 spectrophotometer using KBr pellets. Thermogravimetric analysis (TGA) was carried out on a Netzsch STA 449C system at a heating rate of 5 K min⁻¹ from 40 °C temperature to 800 °C under nitrogen atmosphere in the Al_2O_3

crucibles. Excitation and emission spectra and luminescence lifetime (τ) of the solid samples were recorded on Edinburgh FL920 spectrophotometer using a 450 W xenon lamp as excitation source. The outer luminescent quantum efficiency was measured by an integrating sphere (150 mm diameter, BaSO_4 coating) from Edinburgh FL920 phosphorimeter. The spectra were corrected for variations in the output of the excitation source and in the detector response. The quantum yield can be defined as the integrated intensity of the luminescence signal divided by the integrated intensity of the absorption signal. The absorption intensity was calculated by subtracting the integrated intensity of the light source with the sample in the integrating sphere from the integrated intensity of the light source with a blank sample in the integrating sphere. All the measurements were performed at room temperature.

RESULTS AND DISCUSSION

Characterization of Eu^{3+} @MIL-121. MIL-124 was hydrothermally synthesized using $\text{Ga}(\text{NO}_3)_3 \cdot x\text{H}_2\text{O}$, 1,2,4- H_3btc , and H_2O as reported.⁵³ The experimental PXRD pattern of the synthesized MIL-124 was in good agreement with the simulated one, showing the successful preparation of MIL-124 (Figure 1a). The SEM image of the MIL-124 phase (see Figure S1 in the Supporting Information) shows large crystals with the dimension in the range of 100–250 μm . Representation of the structure of the gallium trimellitate MIL-124 (see Figure S2 in the Supporting Information) shows a layerlike network developing in the (a, c) plane. In the structure,

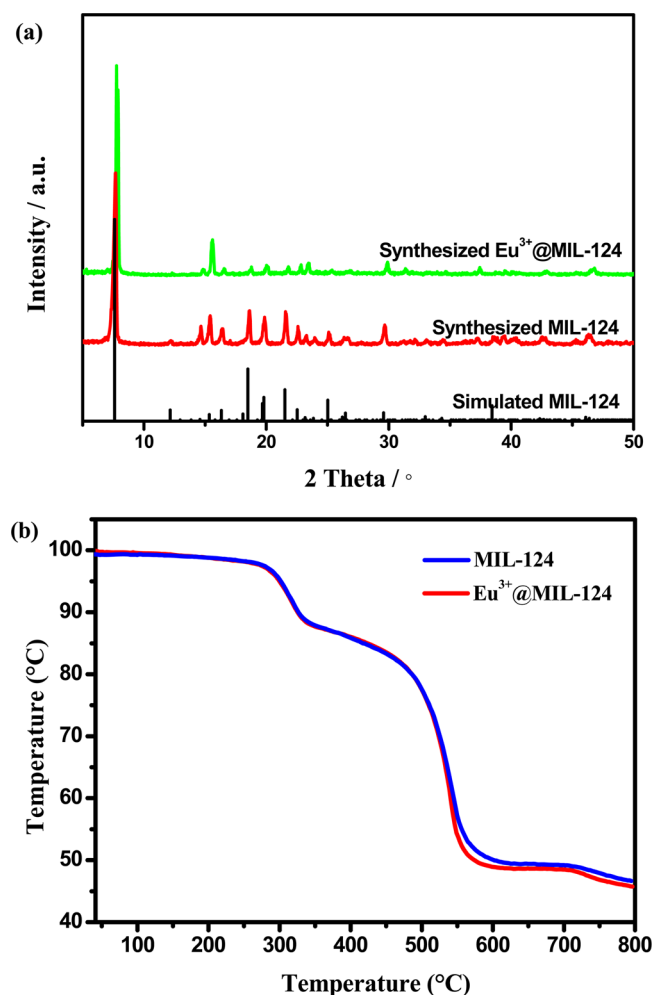


Figure 1. PXRD and TGA of MIL-124 and Eu^{3+} @MIL-124.

adjacent inorganic chains are linked to each other through the carboxylate functions in 1,2 positions of the trimellitate ligand, with a syn-syn bidentate mode bridging the two gallium atoms Ga1 and Ga2. That results a free carboxylate function (4-position), which can be funded in the FTIR spectra of MIL-124 in Figure S3 in the Supporting Information. The broad band at 3000–2500 cm^{-1} is ascribed to the characteristic stretching vibrations of O–H in free carboxylic acid. Beside the peak at 1700 cm^{-1} belongs to $\nu_{\text{C}=\text{OH}_{\text{free}}}$ whereas the peak at 1564 cm^{-1} belongs to $\nu_{\text{C}-\text{O}_{\text{bonded}}}$. Afterward, MIL-124 was immersed in an ethanol solution of EuCl_3 for Eu^{3+} encapsulation by connecting to the free-COOH of MIL-124. As shown in Figure S4, the absorption band of MIL-124 show a significant red-shift (~ 13 nm) after binding to Eu^{3+} ions. This indicates the formation of coordination bonds between the Eu^{3+} and free-COOH of MIL-124.⁴⁰ After introducing Eu^{3+} into the MOF, the compounds can maintain the crystalline integrity, as shown by the PXRD patterns (Figure 1a).

The as-prepared Eu^{3+} @MIL-124 was also monitored by TG analysis from 40 to 800 $^{\circ}\text{C}$ (Figure 1b). The TGA exhibits two events of weight losses in which Eu^{3+} @MIL-124 shows good thermal stability similar to MIL-124. The first step occurs in the range of 250–350 $^{\circ}\text{C}$, which assigns to the partial decomposition of the organic ligand with the removal of the nonbonded CO_2 species. The second weight loss between 450 and 600 $^{\circ}\text{C}$ is attributed to the departure of the remaining organic part together with H_2O coming from the dehydroxylation. The final plateau from 600 $^{\circ}\text{C}$ corresponds to amorphous gallium oxide.

Luminescence Properties of Eu^{3+} @MIL-124. Although free H_3btc ligand shows weak fluorescence emission at 404 nm, the coordination of H_3btc ligand to Ga^{3+} in the MIL-124 gives intense fluorescence emission at 400 nm excitation at 321 nm (see Figure S5 in the Supporting Information), which may be attributed to ligand-to-metal charge transfer (LMCT).⁵⁴ As expected, after postsynthetic functionalization of Eu^{3+} , the emission spectrum of the product exhibits characteristic emission of Eu^{3+} . The sharp lines centered at 580, 593, 615, 653, 701 nm can be ascribed to $^5\text{D}_0 \rightarrow ^7\text{F}_J$ ($J = 0-4$) transitions of Eu^{3+} .^{55,56} Figure 2 shows a very intense $^5\text{D}_0 \rightarrow ^7\text{F}_2$ transition

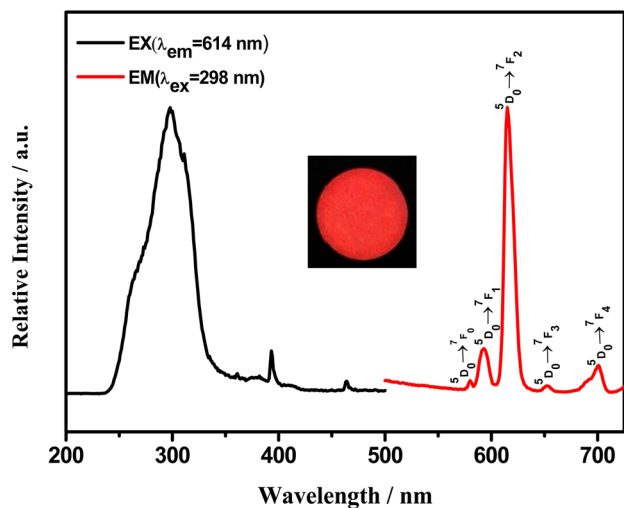


Figure 2. Excitation (black line) and emission (red line) spectra of Eu^{3+} @MIL-124. The inset is the corresponding luminescence picture under UV-light irradiation of 254 nm.

at 615 nm. It is well-known that the $^5\text{D}_0 \rightarrow ^7\text{F}_2$ transition is a typical electric dipole transition. It is very sensitive to the local symmetry of Eu^{3+} , whereas the parity-allowed magnetic dipole transition $^5\text{D}_0 \rightarrow ^7\text{F}_1$ is practically independent of the ions' surroundings. Hence, the intensity ratios $I(^5\text{D}_0/^7\text{F}_2)/I(^5\text{D}_0/^7\text{F}_1)$ (I_{02}/I_{01}) can be considered an indicator for the local environment of the ions. According to the calculated intensity ratio (about 6.3), we concluded that the chemical environment around the Eu^{3+} is in low symmetry.^{9,35,40,57} Under UV-light irradiation, Eu^{3+} @MIL-124 shows strong red luminescence which can be readily observed by naked eye, as shown in the inset of Figure 2, indicating the antenna effect occurs. Moreover, Eu^{3+} @MIL-124 exhibits reasonable long lifetimes (0.40 ms) and quantum yields (8.3%), which are attributed to the effective energy transfer from the ligand to the Eu^{3+} .

We have investigated the luminescence properties of Eu^{3+} @MIL-124 in aqueous solution. As shown in Figure S6 in the Supporting Information, the luminescence intensity of the Eu^{3+} @MIL-124 suspension shows surprisingly little reduction as the time progresses, implying good day-to-day fluorescence stability in aqueous solution. The good stability also can indicate the feasibility of Eu^{3+} @MIL-124 as a fluorescent probe in an aqueous environment, which can be ascribed to the sufficient protection to Eu^{3+} provided by MOF scaffold.⁹

Sensing of Metal Ions. In light of the excellent luminescence and good water stability of Eu^{3+} @MIL-124, we examine the potential application of Eu^{3+} @MIL-124 for detecting metal ions. The as-synthesized sample was simply immersed in an aqueous solution of 0.01 mol L^{-1} MCl_x ($\text{M} = \text{K}^+, \text{Na}^+, \text{Hg}^{2+}, \text{Cd}^{2+}, \text{Ca}^{2+}, \text{Ni}^{2+}, \text{Co}^{2+}, \text{Mn}^{2+}, \text{Cu}^{2+}, \text{Fe}^{2+}, \text{Al}^{3+}, \text{Fe}^{3+}$, respectively). The luminescent properties were recorded and compared in Figure 3. The results revealed that various metal ions display markedly different effects on the luminescence of Eu^{3+} ions.

For example, the luminescence intensity at 615 nm is decreased when Ni^{2+} , Al^{3+} , Na^+ , Co^{2+} , Mn^{2+} , Cu^{2+} , Fe^{2+} , or Fe^{3+} are involved. In the contrast, the interaction with K^+ drastically enhanced the luminescence intensity. The rest of the metal ions

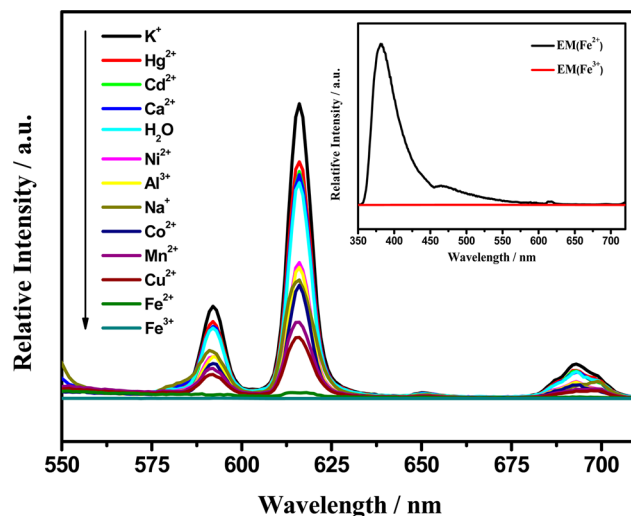


Figure 3. PL spectra of Eu^{3+} @MIL-124 (2 mg) dispersed into different aqueous solution of various metal ions (1×10^{-2} mol L^{-1}). The inset is the PL spectra of Eu^{3+} @MIL-124 dispersed into aqueous solution of Fe^{2+} (blank line) and Fe^{3+} (red line).

(Hg²⁺, Cd²⁺, Ca²⁺) tested did not cause any significant change to the intensity of the Eu³⁺ luminescence. The different quenching effects lead to the changes of emitting color under the UV-light irradiation and the luminescence color changes was completely consistent with the variation tendency of the emission spectra in the inset of Figure 4. For the Fe²⁺ and Fe³⁺

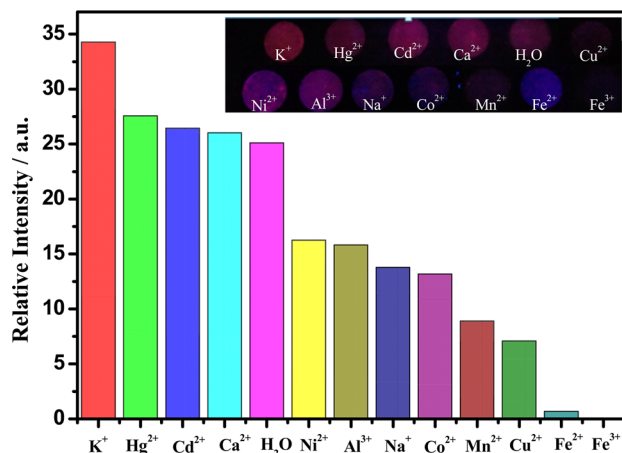


Figure 4. Luminescence intensity of the ⁴D₀-⁷F₂ of Eu³⁺@MIL-124 interacting with different metal ions in 1 × 10⁻² mol L⁻¹ aqueous solution of MCl_n (excited monitored at 298 nm). The inset is the corresponding photographs under UV-light irradiation at 254 nm.

ions, although they all seriously quench the emission of Eu³⁺, their emission colors are different and easy to distinguish under UV light (inset of Figure 4). As shown in the inset of Figure 3, Fe²⁺ can completely quench the emission of Eu³⁺ but remain the emission of MOF, causing the blue light. However, Fe³⁺ ions can not only quench the emission of Eu³⁺ but also have quenching effect on the emission of MOF, which leads the dark under UV-light. And upon the introduction of Fe³⁺ to the mixture of Eu³⁺@MIL-124 and other metal cations, the fluorescence is significantly quenched (see Figure S7 in the Supporting Information). To clear the different degrees of quenching effects on the MOF emission by the Fe²⁺ and Fe³⁺, we immerse the pure MOF in the aqueous solution of Fe²⁺ and Fe³⁺, respectively. As expected, Fe³⁺ totally quench the emission of pure MOF while the Fe²⁺ have no significantly quenching effect showing in Figure S8 in the Supporting Information. Therefore, Eu³⁺@MIL-124 can selectively sense Fe²⁺ and Fe³⁺ ions though the different quenching effects to Eu³⁺ and MOF.

In addition, the quenching effects of M^{Z+} on the luminescence of Eu³⁺@MIL-124 were evaluated by the fluorescence decay time of Eu³⁺. As shown in Table 1, most of the metal ions have no significant effects on the luminescence lifetime of Eu³⁺, whereas Fe²⁺ and Fe³⁺ ions exhibit varying degrees of reduction in the luminescence lifetimes which displays 109.57 μs and undetectable, respectively. This observation agrees well with the responses of luminescence of Eu³⁺@MIL-124 toward various metal ions.

To further prove that the fluorescence quenching by Fe²⁺ and Fe³⁺, concentration-dependent studies in the luminescence properties of Eu³⁺@MIL-124 when Fe²⁺ and Fe³⁺ ions are present were carried out. However, the PL intensity for Fe²⁺ and Fe³⁺-loaded samples are quite different for the Eu³⁺ and MIL-124. As demonstrated in Figure 5a, the emission intensity of the Eu³⁺@MIL-124 suspension declines sharply with the increase of Fe³⁺ concentration from 0 to 500 μM.

Table 1. Response of Luminescence Lifetime of Eu³⁺@MIL-124 toward Aqueous Solutions of Various Metal Ions

metal ions	τ (μs)
K ⁺	315.83
Hg ²⁺	252.30
Cd ²⁺	200.51
Ca ²⁺	204.72
Ni ²⁺	202.88
Al ³⁺	224.96
Na ⁺	263.78
Co ²⁺	226.74
Mn ²⁺	243.68
Cu ²⁺	198.71
Fe ²⁺	109.57
Fe ³⁺	undetectable

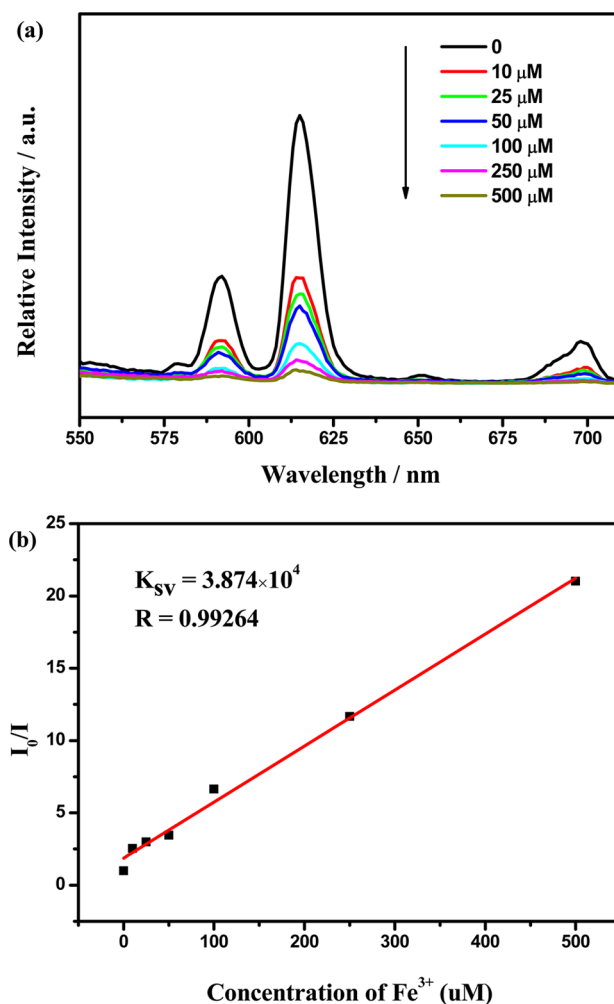


Figure 5. (a) Emission spectra and (b) K_{sv} curve of Eu³⁺@MIL-124 in aqueous solutions in the presence of various concentrations of Fe³⁺ under excitation at 298 nm.

Quantitatively, this quenching effect can be rationalized by the Stern–Volmer equation

$$I_0/I = 1 + K_{sv}[M]$$

where the values I_0 and I are the luminescence intensity of the Eu³⁺@MIL-124 suspension without and with addition of Fe³⁺, respectively, K_{sv} is the quenching constant, $[M]$ is the Fe³⁺ concentration.⁵⁸ On the basis of the experimental data in Figure

Sb, the linear correlation coefficient (R) in the K_{sv} curve of $\text{Eu}^{3+}@MIL-124$ with Fe^{3+} is 0.99264, which suggests that the quenching effect of Fe^{3+} on the luminescence of $\text{Eu}^{3+}@MIL-124$ fits the Stern–Volmer mode well. The K_{sv} value is calculated as 3.874×10^4 , which reveals a strong quenching effect on the $\text{Eu}^{3+}@MIL-124$ luminescence. However, in Figure 6, the luminescence intensity of Eu^{3+} decreases, whereas the

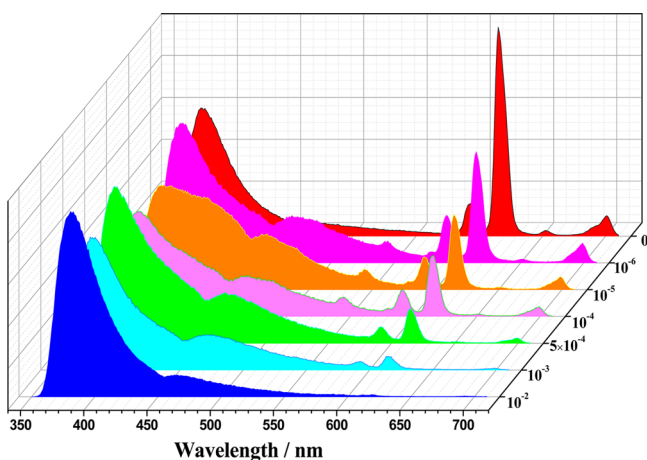


Figure 6. Comparison of luminescence of $\text{Eu}^{3+}@MIL-124$ in aqueous solution in the presence of various concentrations of Fe^{2+} under excitation at 298 nm.

emission of MOF changes a little with the increasing of Fe^{2+} concentration. When the concentration reaches $1 \times 10^{-3} \text{ mol L}^{-1}$, the quenching effect on the luminescence of Eu^{3+} is obvious. When the concentration reaches $1 \times 10^{-2} \text{ mol L}^{-1}$, the luminescence is quenched completely and only the emission of the MOF can be seen.

To make the detection simple and portable, we developed a fluorescence test paper for rapid detection of metal ions. Hence, the sensing of Fe^{2+} and Fe^{3+} in aqueous solution was carried out. The test paper was prepared by immersing a filter paper ($0.5 \times 1.0 \text{ cm}^2$) in the ethanol of $\text{Eu}^{3+}@MIL-124$ and drying it at room temperature.¹¹ For the detection of Fe^{2+} and Fe^{3+} in water, we immersed the test paper in the aqueous solution of metal ions for 1 min and then exposed it to air for drying. As shown in Figure 7a, under the irradiation of UV light of 254 nm, the fluorescent colors of the test paper changed from red to

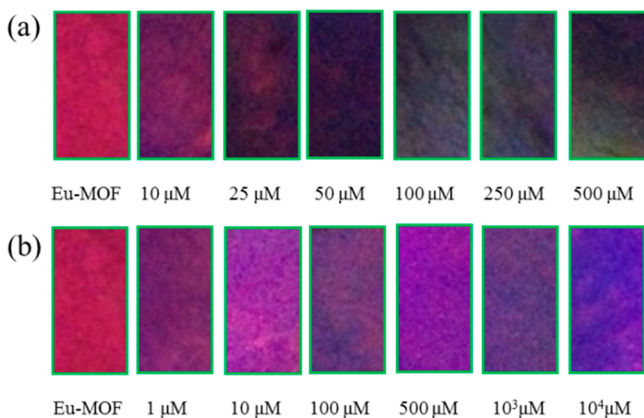


Figure 7. Optical images of the $\text{Eu}^{3+}@MIL-124$ test paper after immersion into solution with different concentrations of (a) Fe^{3+} and (b) Fe^{2+} for 1 min.

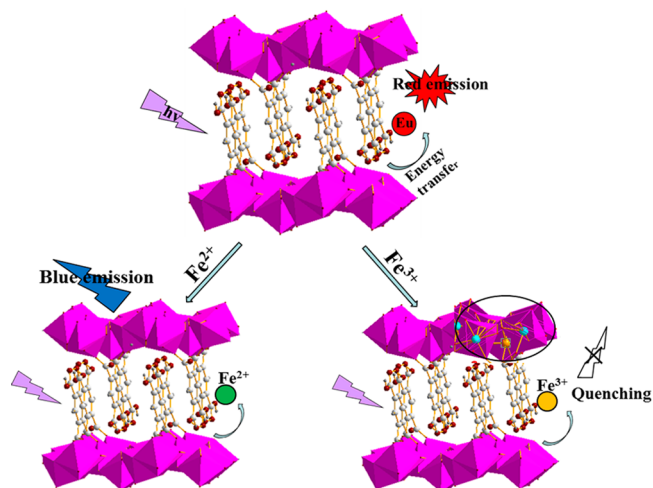
dark red, faint dark red, and finally black with the increase of Fe^{3+} . The least concentration of detection for Fe^{3+} by fluorescence test paper is $50 \mu\text{M}$. At the same time, when immersing the test paper in various concentration of Fe^{2+} aqueous solution, the color changed from red to blue showing in Figure 7b, which indicates obvious different with Fe^{3+} . Considering the results above, we can distinguish the colors of different intensities by our naked eyes.

To the date, the quenching effect on luminescence of MOFs by metal ions originates from three approaches: (1) the interaction between metal ions and organic ligands;⁵⁹ (2) the collapse of the crystal structure,⁶⁰ (3) the ions exchange between central metal ions of MOFs and the targeted ions.^{61,9} Hereon, the possible sensing mechanism for the luminescence quenching by the metal ions has been further investigated. The power XRD was employed to study on the structural data of the original and exchanged compounds. As shown in Figure S9 in the Supporting Information, the power XRD for all the metal ions are similar to that of $\text{Eu}^{3+}@MIL-124$, suggesting that the basic frameworks remain unchanged. Considering other mechanisms, we speculate that the remarkable quenching effect of $\text{Eu}^{3+}@MIL-124$ by Fe^{3+} and Fe^{2+} results from the transformation of the patented framework MIL-124 (Ga) to MIL-124 (Fe) via the cation exchange. However, the MIL-124 (Fe) were synthesized unsuccessfully as the XRD patterns of Fe-MOF were different with MIL-124 (Ga) (see Figure S10 in the Supporting Information). Therefore, the quenching effect to Eu^{3+} should be attributed to the interaction between metal ions and organic ligands. The detailed ICP studies (see Table S1 in the Supporting Information) of Fe^{2+} and Fe^{3+} involving $\text{Eu}^{3+}@MIL-124$ indicated the different quenching effect to the illuminant bodies by Fe^{2+} and Fe^{3+} . The quenching effect of $\text{Eu}^{3+}@MIL-124$ by Fe^{3+} can attribute to the partial replacement of Ga^{3+} and substitution of Eu^{3+} , whereas substitution of Eu^{3+} is the main reason for the fluorescence quenching by Fe^{2+} (Scheme 1).

Sensing for Anions and Organic Small Molecule.

Simultaneously, various anions were selected to carry out the anion-sensing function by immersing $\text{Eu}^{3+}@MIL-124$ in different anion aqueous solutions (anion = F^- , Cl^- , Br^- , I^- , NO_3^- , SO_4^{2-} , CrO_4^{2-} , $\text{Cr}_2\text{O}_7^{2-}$). The original framework

Scheme 1. Simplified Schematic Illustration of Luminescence Quenching Mechanism of $\text{Eu}^{3+}@MIL-124$ by Fe^{3+} and Fe^{2+} Ion



almost kept unchanged as confirmed by PXRD (see Figure S11 in the Supporting Information). The luminescent measurements illustrate that the difference of anions has a great influence in the luminescence intensity of $\text{Eu}^{3+}@MIL-124$ as shown in Figure 8a. Remarkably, $\text{Cr}_2\text{O}_7^{2-}$ has the largest

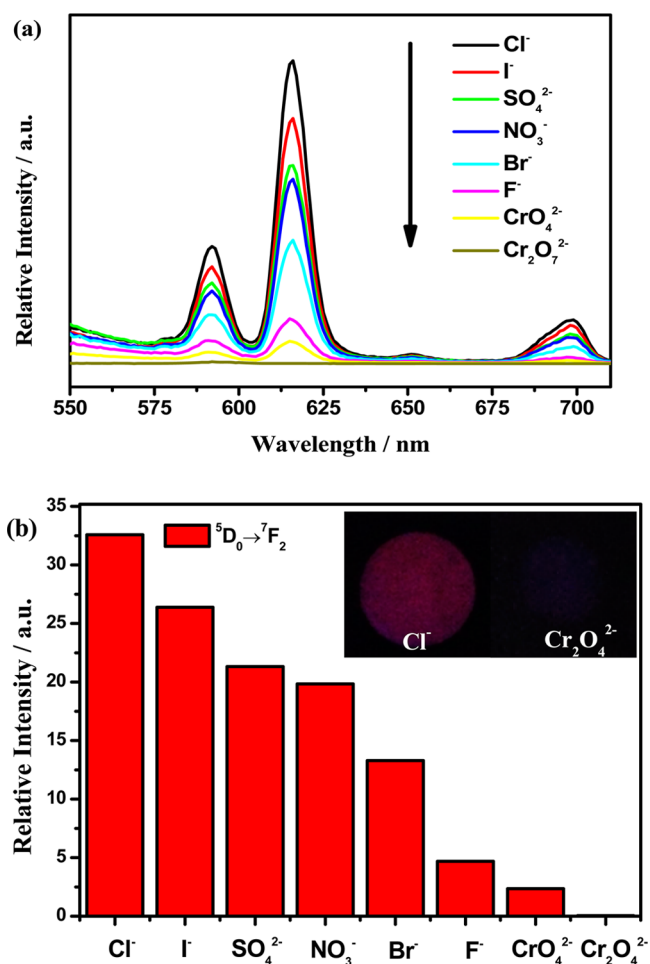


Figure 8. (a) PL spectra of $\text{Eu}^{3+}@MIL-124$ (2 mg) and (b) the luminescence intensity of the ${}^4\text{D}_0 \rightarrow {}^7\text{F}_2$ of $\text{Eu}^{3+}@MIL-124$ dispersed into different aqueous solution of various anions (1×10^{-2} mol L^{-1}).

quenching effect on the luminescent emission which leads to a dark emission (inset of Figure 8b) and has reduced the luminescent lifetime of $\text{Eu}^{3+}@MIL-124$ from 0.4 to 0.1 ms (see Figure S12 in the Supporting Information). The fluorescence of $\text{Eu}^{3+}@MIL-124$ was gradually quenched as the $\text{Cr}_2\text{O}_7^{2-}$ concentration increased (see Figure S13a in the Supporting Information). The quenched fluorescence intensity (I_0/I) of $\text{Eu}^{3+}@MIL-124$ has a good linear relationship to the $\text{Cr}_2\text{O}_7^{2-}$ concentration ($R = 0.99343$) in the concentration range of 10–500 μM $\text{Cr}_2\text{O}_7^{2-}$ (see Figure S13b in the Supporting Information). $\text{Eu}^{3+}@MIL-124$ shows highly selective for $\text{Cr}_2\text{O}_7^{2-}$ (detection limit, 0.15 μM).

Hence, we also examine the potential of $\text{Eu}^{3+}@MIL-124$ for the sensing of organic small molecules because of their environmental biological hazards.^{62–65} Before the luminescent measurements, PXRD patterns illustrate good solvent-stability of $\text{Eu}^{3+}@MIL-124$ treated by different solvents (see Figure S14 in the Supporting Information). As shown in Figure 9a, the PL spectra are significantly dependent on the solvent molecules, particularly in the case of acetone, which exhibit clearly

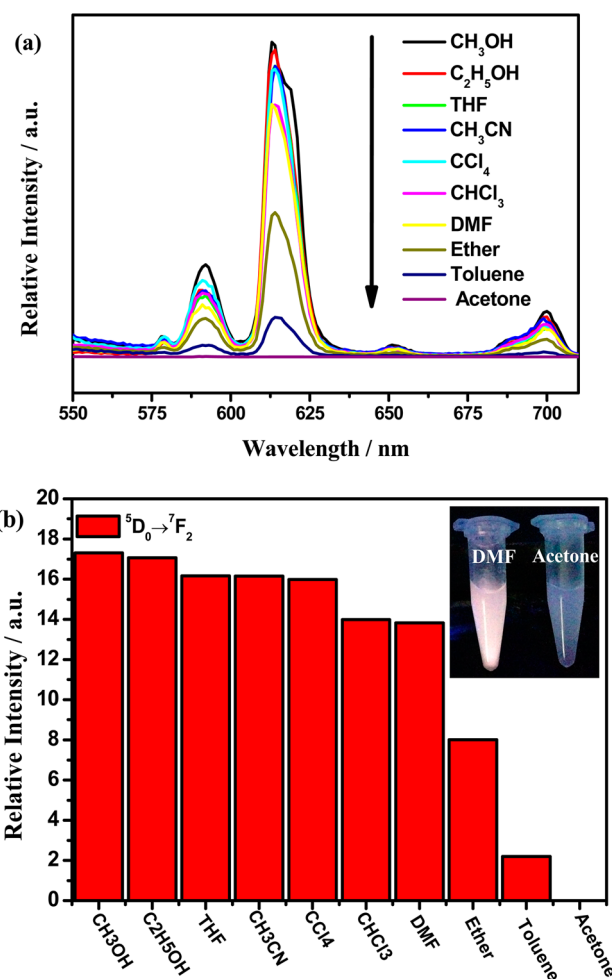


Figure 9. (a) PL spectra and (b) the luminescence intensity of the ${}^4\text{D}_0 \rightarrow {}^7\text{F}_2$ of $\text{Eu}^{3+}@MIL-124$ dispersed into different organic small molecules.

quenching effects. The remarkable quenching effect can be further confirmed by the photograph of the $\text{Eu}^{3+}@MIL-124$ suspension under UV light irradiation (Figure 9b). When immersing different quantities (6–2 mg) of $\text{Eu}^{3+}@MIL-124$ in 2 mL acetone, the emission of Eu^{3+} results in a dramatic decreased luminescence intensity (see Figure S15a in the Supporting Information). As a result, with the decrease in $\text{Eu}^{3+}@MIL-124$, the fluorescence color changed from purplish red to dark under a 254 nm UV lamp (inset in Figure S15b in the Supporting Information), which can be easily distinguished by the naked eyes.

To date, the mechanisms for such quenching effects of anions and small solvent molecules are still not very clear. Nevertheless, the influence of the anions on antenna effect definitely plays an important role, since the antenna effect is crucial to determine the emission of lanthanide. To deeply understand the luminescence quenching effects by $\text{Cr}_2\text{O}_7^{2-}$, the UV–vis spectra of anions themselves are measured (see Figure S16 in the Supporting Information). It is obvious that the absorption peak of ligands within $\text{Eu}^{3+}@MIL-124$ is almost masked by the wide absorption of $\text{Cr}_2\text{O}_7^{2-}$. The $\text{Cr}_2\text{O}_7^{2-}$ competes with the organic ligand for absorption of light energy and hence reduces the amount of light absorbed by the ligand thereby reducing the efficiency of energy transfer from the ligand to the lanthanide ions. The luminescent signal induced

by organic small molecules can be partially attributed to the UV–vis absorption (see Figure S17 in the Supporting Information). The result indicates that the absorption band of acetone partially overlaps with the absorption band of Eu^{3+} @MIL-124, which has reduced the absorption of light by organic ligand and affected the energy transformation from MOF to Eu^{3+} .

CONCLUSIONS

In summary, a layerlike MOF (MIL-124, or $\text{Ga}_2(\text{OH})_4(\text{C}_9\text{O}_6\text{H}_4)_n$) has been prepared and chosen as a parent compound to encapsulate Eu^{3+} cations by one uncoordinated carbonyl group in its pores. The characters of PXRD, TGA, and luminescent measurements demonstrate that this framework can be explored as potential multifunctional luminescent material for sensing of metal ions, anions, and organic small molecules, especially for Fe^{3+} and Fe^{2+} . Studying of the luminescence properties reveals that Eu^{3+} @MIL-124 can develop as a highly selective and sensitive probe for detection of Fe^{3+} (detection limit, $0.28 \mu\text{M}$) and Fe^{2+} ions through fluorescence quenching of Eu^{3+} and MOF. The colors of fluorescence test paper immersing in different intensities of Fe^{3+} and Fe^{2+} can be observed changing from red to black or blue, respectively, by naked eyes under the irradiation of UV light. Further study and speculation of the mechanism illustrate that the interaction between metal ions and organic ligand lead to the quenching effect of Eu^{3+} @MIL-124. Hence, we also examine the potential application of Eu^{3+} @MIL-124 for the sensing of anions and small organic molecules, which show an excellent selective for $\text{Cr}_2\text{O}_7^{2-}$ (detection limit, $0.15 \mu\text{M}$) and acetone. The present results may provide a facile route to design luminescence Ln-MOF for sensing and further studies are currently under way.

ASSOCIATED CONTENT

Supporting Information

SEM image, structure representation, FTIR spectra, PXRD patterns, and luminescence spectra. This material is available free of charge via the Internet at <http://pubs.acs.org>.

AUTHOR INFORMATION

Corresponding Author

* Phone: +86-21-65984663. Fax: +86-21-65981097. E-mail: byan@tongji.edu.cn.

Author Contributions

[‡]The manuscript was written through contributions of all authors. All authors have given approval to the final version of the manuscript. These authors contributed equally.

Notes

The authors declare no competing financial interest.

ACKNOWLEDGMENTS

This work was supported by the National Natural Science Foundation of China (20971100, 91122003) and Developing Science Funds of Tongji University.

REFERENCES

- (1) Praveen, L.; Reddy, M. L. P.; Varma, R. L. Dansyl-Styrylquinoline Conjugate as Divalent Iron Sensor. *Tetrahedron Lett.* **2010**, *51*, 6626–6629.
- (2) de Silva, A. P.; Gunaratne, H. Q. N.; Gunlaugsson, T.; Huxley, A. J. M.; McCoy, C. P.; Rademacher, J. T.; Rice, T. E. Signaling

Recognition Events with Fluorescent Sensors and Switches. *Chem. Rev.* **1997**, *97*, 1515–1566.

- (3) Moon, S. Y.; Cha, N. R.; Kim, Y. H.; Chang, S. K. New Hg^{2+} -Selective Chromo- and Fluoroionophore Based upon 8-Hydroxyquinoline. *J. Org. Chem.* **2004**, *69*, 181–183.

- (4) Zhan, H.; Wang, Q. L.; Jiang, Y. B. 8-Methoxyquinoline Based Turn-on Metal Fluoroionophores. *Tetrahedron Lett.* **2007**, *48*, 3959–3962.

- (5) Prodi, L.; Bargossi, C.; Montalti, M.; Zaccheroni, N.; Su, N.; Bradshaw, J. S.; Izatt, R. M.; Savage, P. B. An Effective Fluorescent Chemosensor for Mercury Ions. *J. Am. Chem. Soc.* **2000**, *122*, 6769–6770.

- (6) Matsumiya, H.; Iki, N.; Miyano, S. Sulfonylecalix[4]-arenetetrasulfonate as Pre-Column Chelating Reagent for Selective Determination of Aluminum(III), Iron(III), and Titanium(IV) by Ion-Pair-Reversed-Phase High-Performance Liquid Chromatography with Spectrophotometric Detection. *Talanta* **2004**, *62*, 337–342.

- (7) Liu, X.; Theil, E. C. Ferritins: Dynamic Management of Biological Iron and Oxygen Chemistry. *Acc. Chem. Res.* **2005**, *38*, 167–175.

- (8) Gray, H. B.; Winkler, J. R. Electron Transfer in Proteins. *Annu. Rev. Biochem.* **1996**, *65*, 537–561.

- (9) Zhou, Y.; Chen, H. H.; Yan, B. An Eu^{3+} Post-Functionalized Nanosized Metal–Organic Framework for Cation-Exchange-Based Fe^{3+} -Sensing in an Aqueous Environment. *J. Mater. Chem. A* **2014**, *2*, 13691–13697.

- (10) Yang, C. X.; Ren, H. B.; Yan, X. P. Fluorescent Metal–Organic Framework MIL-53(Al) for Highly Selective and Sensitive Detection of Fe^{3+} in Aqueous Solution. *Anal. Chem.* **2013**, *85*, 7441–7446.

- (11) Chen, Z.; Sun, Y. W.; Zhang, L. L.; Sun, D.; Liu, F.; Meng, Q. G.; Wang, R. M.; Sun, D. F. A Tubular Europium–Organic Framework Exhibiting Selective Sensing of Fe^{3+} and Al^{3+} over Mixed Metal Ions. *Chem. Commun.* **2013**, *49*, 11557–11559.

- (12) Zheng, M.; Tan, H. Q.; Xie, Z. G.; Zhang, L. G.; Jing, X. B.; Sun, Z. C. Fast Response and High Sensitivity Europium Metal Organic Framework Fluorescent Probe with Chelating Terpyridine Sites for Fe^{3+} . *ACS Appl. Mater. Interface* **2013**, *5*, 1078–1083.

- (13) Lu, Y.; Yan, B.; Liu, J. L. Nanoscale Metal–Organic Frameworks as Highly Sensitive Luminescent Sensors for Fe^{2+} in Aqueous Solution and Living Cells. *Chem. Commun.* **2014**, *50*, 9969–9972.

- (14) Chen, J. L.; Zhuo, S. J.; Wu, Y. Q.; Fang, F.; Li, L.; Zhu, C. Q. High Selective Determination of Iron(II) by Its Enhancement Effect on the Fluorescence of Pyrene-Tetramethylpiperidyl (TEMPO) as a Spin Fluorescence Probe. *Spectrochim. Acta, Part A* **2006**, *63*, 438–443.

- (15) Li, P.; Fang, L. B.; Zhou, H.; Zhang, W.; Wang, X.; Li, N.; Zhong, H. B.; Tang, B. A New Ratiometric Fluorescent Probe for Detection of Fe^{2+} with High Sensitivity and Its Intracellular Imaging Applications. *Chem.—Eur. J.* **2011**, *17*, 10520–10523.

- (16) Li, L. J.; Tang, S. F.; Wang, C.; Lv, X. X.; Jiang, M.; Wu, H. Z.; Zhao, X. B. High Gas Storage Capacities and Stepwise Adsorption in a UiO Type Metal–Organic Framework incorporating Lewis Basic Bipyridyl Sites. *Chem. Commun.* **2014**, *50*, 2304–2307.

- (17) Gándara, F.; Furukawa, H.; Lee, S.; Yaghi, O. M. High Methane Storage Capacity in Aluminum Metal–Organic Frameworks. *J. Am. Chem. Soc.* **2014**, *136*, 5271–5274.

- (18) Wang, Y. L.; Tan, C. H.; Sun, Z. H.; Xue, Z. Z.; Zhu, Q. L.; Shen, C. J.; Wen, Y. H.; Hu, S. M.; Wang, Y.; Sheng, T. L.; Wu, X. T. Effect of Functionalized Groups on Gas-Adsorption Properties: Syntheses of Functionalized Microporous Metal–Organic Frameworks and Their High Gas-Storage Capacity. *Chem.—Eur. J.* **2014**, *20*, 1341–1348.

- (19) He, Y. B.; Zhou, W.; Qian, G. D.; Chen, B. L. Methane Storage in Metal–Organic Frameworks. *Chem. Soc. Rev.* **2014**, *43*, 5657–5678.

- (20) Roy, S.; Chakraborty, A.; Maji, T. K. Lanthanide–Organic Frameworks for Gas Storage and as Magneto-Luminescent Materials. *Coord. Chem. Rev.* **2014**, *273–274*, 139–164.

- (21) Qiu, S. L.; Xue, M.; Zhu, G. S. Metal–Organic Framework Membranes: from Synthesis to Separation Application. *Chem. Soc. Rev.* **2014**, *43*, 6116–6140.

- (22) Yin, H. M.; Wang, J. Q.; Xie, Z.; Yang, J. H.; Bai, J.; Lu, J. M.; Zhang, Y.; Yin, D. H.; Lin, J. Y. S. A Highly Permeable and Selective Amino-Functionalized MOF CAU-1 Membrane for CO₂-N₂ Separation. *Chem. Commun.* **2014**, *50*, 3699–3701.
- (23) Xie, Z. Z.; Li, T.; Rosi, N. L.; Carreon, M. A. Alumina-Supported Cobalt-Adeninate MOF Membranes for CO₂/CH₄ Separation. *J. Mater. Chem. A* **2014**, *2*, 1239–1241.
- (24) Rodenas, T.; van Dalen, M.; García Pérez, E.; Serra Crespo, P.; Zornoza, B.; Kapteijn, F.; Gascon, J. Visualizing MOF Mixed Matrix Membranes at the Nanoscale: Towards Structure-Performance Relationships in CO₂/CH₄ Separation Over NH₂-MIL-53(Al)@PI. *Adv. Funct. Mater.* **2014**, *24*, 249–256.
- (25) Kozachuk, O.; Luz, I.; Xamena, F. X. L.; Noei, H.; Kauer, M.; Albada, H. B.; Bloch, E. D.; Marler, B.; Wang, Y. M.; Muhler, M.; Fischer, R. A. Asymmetric Palladium-Catalyzed Allylic Alkylation Using Dialkylzinc Reagents: A Remarkable Ligand Effect. *Angew. Chem., Int. Ed.* **2014**, *53*, 7068–7073.
- (26) Manna, K.; Zhang, T.; Lin, W. B. Postsynthetic Metalation of Bipyridyl-Containing Metal–Organic Frameworks for Highly Efficient Catalytic Organic Transformations. *J. Am. Chem. Soc.* **2014**, *136*, 6566–6569.
- (27) Jayaramulu, K.; Narayanan, R. P.; George, S. J.; Maji, T. K. Luminescent Microporous Metal–Organic Framework with Functional Lewis Basic Sites on the Pore Surface: Specific Sensing and Removal of Metal Ions. *Inorg. Chem.* **2014**, *51*, 10089–10091.
- (28) Hao, Z. M.; Song, X. Z.; Zhu, M.; Meng, X.; Zhao, S. N.; Su, S. Q.; Yang, W. T.; Song, S. Y.; Zhang, H. J. One-Dimensional Channel-Structured Eu-MOF for Sensing Small Organic Molecules and Cu²⁺ ion. *J. Mater. Chem. A* **2013**, *1*, 11043–11050.
- (29) Kreno, L. E.; Leong, K.; Farha, O. K.; Allendorf, M.; Van Duyne, R. P.; Hupp, J. T. Metal–Organic Framework Materials as Chemical Sensors. *Chem. Rev.* **2012**, *112*, 1105–1125.
- (30) Ma, D. X.; Li, B. Y.; Zhou, X. J.; Zhou, Q.; Liu, K.; Zeng, G.; Li, G. H.; Shi, Z.; Feng, S. H. A Dual Functional MOF as a Luminescent Sensor for Quantitatively Detecting the Concentration of Nitrobenzene and Temperature. *Chem. Commun.* **2013**, *49*, 8964–8966.
- (31) Zhang, M.; Feng, G.; Song, Z. G.; Zhou, Y. P.; Chao, H. Y.; Yuan, D. Q.; Tan, T. T. Y.; Guo, Z. G.; Hu, Z. G.; Tang, B. Z.; Liu, B.; Zhao, D. Two-Dimensional Metal–Organic Framework with Wide Channels and Responsive Turn-on Fluorescence for the Chemical Sensing of Volatile Organic Compounds. *J. Am. Chem. Soc.* **2014**, *136*, 7241–7244.
- (32) Bhattacharyya, S.; Chakraborty, A.; Jayaramulu, K.; Hazra, A.; Maji, T. K. A Bimodal Anionic MOF: Turn-Off Sensing of Cu^{II} and Specific Sensitization of Eu^{III}. *Chem. Commun.* **2014**, *50*, 13567–13570.
- (33) Vermeulen, N. A.; Karagiari, O.; Sarjeant, A. A.; Stern, C. L.; Hupp, J. T.; Farha, O. K.; Stoddart, J. F. Aromatizing Olefin Metathesis by Ligand Isolation inside a Metal–Organic Framework. *J. Am. Chem. Soc.* **2013**, *135*, 14916–14919.
- (34) Bernini, M. C.; Fairen-Jimenez, D.; Pasinetti, M.; Ramirez-Pastor, A. J.; Snurr, R. Q. Screening of Bio-Compatible Metal–Organic Frameworks as Potential Drug Carriers Using Monte Carlo Simulations. *J. Mater. Chem. B* **2014**, *2*, 766–774.
- (35) Duan, T. W.; Yan, B. Hybrids Based on Lanthanide Ions Activated Yttrium Metal–Organic Frameworks: Functional Assembly, Polymer Film Preparation and Luminescence Tuning. *J. Mater. Chem. C* **2014**, *2*, 5098–5104.
- (36) Chen, B. L.; Wang, L. B.; Qian, G. D. A Luminescent Metal–Organic Framework with Lewis Basic Pyridyl Sites for the Sensing of Metal Ions. *Angew. Chem., Int. Ed.* **2009**, *48*, 500–503.
- (37) Das, M. C.; Qian, G. D.; Chen, B. L. A Zn₄O-Containing Doubly Interpenetrated Porous Metal–Organic Framework for Photocatalytic Decomposition of Methyl Orange. *Chem. Commun.* **2011**, *47*, 11715–11717.
- (38) Chen, B. L.; Yang, Y.; Qian, G. D. Luminescent Open Metal Sites within a Metal–Organic Framework for Sensing Small Molecules. *Adv. Mater.* **2007**, *19*, 1693–1696.
- (39) Xu, H.; Liu, F.; Chen, B. L.; Qian, G. D. A Luminescent Nanoscale Metal–Organic Framework for Sensing of Nitroaromatic Explosives. *Chem. Commun.* **2011**, *47*, 3153–3155.
- (40) Hao, J. N.; Yan, B. Highly Sensitive and Selective Fluorescent Probe for Ag⁺ Based on a Eu³⁺ Post-Functionalized Metal–Organic Framework in Aqueous Media. *J. Mater. Chem. A* **2014**, *2*, 18018–18025.
- (41) Zhao, B.; Gao, H. L.; Chen, X. Y.; Cheng, P. A Promising MgII-Ion-Selective Luminescent Probe: Structures and Properties of Dy–Mn Polymers with High Symmetry. *Chem.—Eur. J.* **2006**, *12*, 149–158.
- (42) Zhao, B.; Chen, X. Y.; Cheng, P. Coordination Polymers Containing 1D Channels as Selective Luminescent Probes. *J. Am. Chem. Soc.* **2004**, *126*, 15394–15395.
- (43) Luo, F.; Batten, S. R. Metal–Organic Framework (MOF): Lanthanide(III)-Doped Approach for Luminescence Modulation and Luminescent Sensing. *Dalton Trans.* **2010**, *39*, 4485–4488.
- (44) Lu, W. G.; Jiang, L.; Feng, X. L.; Lu, T. B. Three-Dimensional Lanthanide Anionic Metal–Organic Frameworks with Tunable Luminescent Properties Induced by Cation Exchange. *Inorg. Chem.* **2009**, *48*, 6997–6999.
- (45) Liu, W. S.; Jiao, T. Q.; Tan, M. Y. Lanthanide Coordination Polymers and Their Ag⁺-Modulated Fluorescence. *J. Am. Chem. Soc.* **2004**, *126*, 2280–2281.
- (46) Liu, S.; Xiang, Z. H.; Hu, Z.; Zheng, X. P.; Cao, D. P. Zeolitic Imidazolate Framework-8 as a Luminescent Material for the Sensing of Metal Ions and Small Molecules. *J. Mater. Chem.* **2011**, *21*, 6649–6653.
- (47) Wang, Q. M.; Tan, C. L. Luminescent Cu²⁺ Probes Based on Rare-Earth (Eu³⁺ and Tb³⁺) Emissive Transparent Cellulose Hydrogels. *Anal. Chim. Acta* **2011**, *708*, 111–115.
- (48) Xiao, Y. Q.; Cui, Y. J.; Zheng, Q.; Xiang, S. C.; Qian, G. D.; Chen, B. L. A Microporous Luminescent Metal–Organic Framework for Highly Selective and Sensitive Sensing of Cu²⁺ in Aqueous Solution. *Chem. Commun.* **2010**, *46*, 5503–5505.
- (49) Cai, S. L.; Zheng, S. R.; Fan, J.; Xiao, T. T.; Tan, J. B.; Zhang, W. G. A New Sensor Based on Luminescent Terbium–Organic Framework for Detection of Fe³⁺ in Water. *Inorg. Chem. Commun.* **2011**, *14*, 937–939.
- (50) Chen, B. L.; Wang, L. B.; Zapata, F.; Qian, G. D.; Lobkovsky, E. B. A Luminescent Microporous Metal–Organic Framework for the Recognition and Sensing of Anions. *J. Am. Chem. Soc.* **2008**, *130*, 6718–6719.
- (51) Lee, T.; Lee, H. L.; Tsai, M. H.; Cheng, S. L.; Lee, S. W.; Hu, J. C.; Chen, L. T. A Biomimetic Tongue by Photoluminescent Metal–Organic Frameworks. *Biosens. Bioelectron.* **2013**, *43*, 56–62.
- (52) Yang, W. T.; Bai, Z. Q.; Shi, W. Q.; Yuan, L. Y.; Tian, T.; Chai, Z. F.; Wang, H.; Sun, Z. M. MOF-76: From a Luminescent Probe to Highly Efficient U^{VI} Sorption Material. *Chem. Commun.* **2013**, *49*, 10415–10417.
- (53) Hajjar, R.; Christophe, V.; Loiseau, T.; Guillou, N.; Marrot, J.; Férey, G.; Margiolaki, I.; Fink, G.; Morais, C.; Taulelle, F. ⁷¹Ga Slow-CTMAS NMR and Crystal Structures of MOF-Type Gallium Carboxylates with Infinite Edge-Sharing Octahedra Chains (MIL-120 and MIL-124). *Chem. Mater.* **2011**, *23*, 39–47.
- (54) Cui, Y. J.; Yue, Y. F.; Qian, G. D.; Chen, B. L. Luminescent Functional Metal–Organic Frameworks. *Chem. Rev.* **2012**, *112*, 1126–1162.
- (55) Zhou, Y.; Yan, B. RE₂(MO₄)₃:Ln³⁺ (RE = Y, La, Gd, Lu; M = W, Mo; Ln = Eu, Sm, Dy) Microcrystals: Controlled Synthesis, Microstructure and Tunable Luminescence. *CrystEngComm* **2013**, *15*, 5694–5702.
- (56) He, X. H.; Yan, B. A Novel Sc³⁺-Containing Fluoride Host Material for Down- and Up-Conversion Luminescence. *J. Mater. Chem. C* **2013**, *1*, 3910–3912.
- (57) Liu, Y. Y.; Decadt, R.; Bogaerts, T.; Hemelsoet, K.; Kaczmarek, A. M.; Poelman, D.; Waroquier, M.; Van Speybroeck, V.; Van Deun, R.; Van Der Voort, P. Bipyridine-Based Nanosized Metal–Organic Framework with Tunable Luminescence by a Postmodification with

Eu(III): An Experimental and Theoretical Study. *J. Phys. Chem. C* **2013**, *117*, 11302–11310.

(58) Thomas, S. W.; Joly, G. D.; Swager, T. M. Chemical Sensors Based on Amplifying Fluorescent Conjugated Polymers. *Chem. Rev.* **2007**, *107*, 1339–1386.

(59) Tang, Q.; Liu, S. X.; Liu, Y. W.; Miao, J.; Li, S. J.; Zhang, L.; Shi, Z.; Zheng, Z. P. Highly Selective Luminescent Sensing of Fluoride and Organic Small-Molecule Pollutants Based on Novel Lanthanide Metal–Organic Frameworks. *Inorg. Chem.* **2013**, *52*, 2799–2801.

(60) Dang, S.; Ma, E.; Sun, Z. M.; Zhang, H. J. A Layer-Structured Eu-MOF as a Highly Selective Fluorescent Probe for Fe³⁺ Detection through a Cation-Exchange Approach. *J. Mater. Chem.* **2012**, *22*, 16920–16926.

(61) Yang, C. X.; Ren, H. B.; Yan, X. P. Fluorescent Metal–Organic Framework MIL-53(Al) for Highly Selective and Sensitive Detection of Fe³⁺ in Aqueous Solution. *Anal. Chem.* **2013**, *85*, 7441–7446.

(62) Zhou, J. M.; Shi, W.; Li, H. M.; Li, H.; Cheng, P. Experimental Studies and Mechanism Analysis of High-Sensitivity Luminescent Sensing of Pollutational Small Molecules and Ions in Ln₄O₄ Cluster Based Microporous Metal–Organic Frameworks. *J. Phys. Chem. C* **2014**, *118*, 416–426.

(63) McDonald, R. W.; Ikonou, M. G.; Paton, D. W. Historical Inputs of PCDDs, PCDFs, and PCBs to a British Columbia Interior Lake: The Effect of Environmental Controls on Pulp Mill Emissions. *Environ. Sci. Technol.* **1998**, *32*, 331–337.

(64) Alcock, R. E.; Jones, K. C.; McLachlan, M. S.; Johnston, A. E. Response to Comment on “Evidence for the Presence of PCDD/Fs in the Environment Prior 1900 and Further Studies on Their Temporal Trends. *Environ. Sci. Technol.* **1999**, *33*, 206–207.

(65) Jones, K. C.; de Voigt, P. Persistent Organic Pollutants (POPs): State of the Science. *Environ. Pollut.* **1999**, *100*, 209–221.